Spin-Polarized Electron Transfer in Multilayers with Different Types of Rough Interfaces

A.H. Ramezani[1], S. Hoseinzadeh[2,3], Z.H. Ebrahiminejad[1], S.F. Masoudi[4] and A. Hashemizadeh[5]

Abstract

In this study, the influence of interfacial roughness of multilayers structures on spin filter tunneling is investigated at low biases as a function of interfacial roughness type. The results show that the roughness causes the reduction of resonant tunneling, maximum achievable tunneling magneto resistance (TMR), and spin-filtering efficiency of tunneling structures. Based on the numerical results, decreasing the electronic devices' efficiency is straight related to roughening of interfacial. Additionally, the effect of different temperatures is investigated on the spin polarization (SP). The values of SP decreased sensibly by increasing the temperature.

Keywords Spin-dependent tunneling · Rough interfacial · Spin-filtering efficiency

1 Introduction

Spin-dependent tunneling through magnetic tunnel structures has recently aroused enormous interest and developed in various ranges of research field [1–5]. The potential advantage of using the electron spins to both store and transfer information has motivated researchers into magnetic tunnel junctions (MTJs) [6]. The barrier height and the thickness of magnetic multilayers play a critical role in the efficiency of electron spin polarization [7–10]. Based on the reported experimental results [3, 11], it is evident that the interfacial roughness of magnetic tunnel junctions can strongly affect the related electron transport quantities such as tunneling magneto resistance (TMR) and the degree of spin polarization [12–18]. The various methods have been proposed to model interfacial roughness in heterojunctions theoretically [12, 13]. In our recent work, the influence of interfacial roughness was studied on the electronic properties of MTJs. These structures consist of a nonmagnetic metal (NM) layer between two ferromagnetic semiconductor (FMS) barriers which was sandwiched between two NM layers. The calculation was carried out at zero temperature [12]. In the present study, the effect of types of rough interfaces has been studied on the electron transport through the mentioned MTJs. In order to make a comparison between our results and experimental works, the two rough interfaces were produced by using the two standard models of deposition, i.e., random deposition (RD) and ballistic deposition (BD) models. For growth, the interfaces/surfaces by using RD model, often a flat substrate, is considered and each particle falls vertically till it reaches to a random site on the substrate. Therefore, the height of the randomly chosen site (column) increases by one. There is no priority for deposition and therefore, there is no correlation among the columns, thus the surfaces grow independently. But in the BD model, the highest site, in comparison with the nearest neighbors, is selected. And, the particles, which fall vertically on the substrate, stick to the aggregation or the substrate in the first contact. Therefore, some parts of interfaces/surfaces are vacant permanently which results to generation of the porous surfaces and the correlation extends along the surface [19–29].

Email A. H. Ramezani
ramezani.1972@gmail.com

Email S. Hoseinzadeh
Hoseinzadeh.siamak@gmail.com

[1] Department of Physics, West Tehran Branch, Islamic Azad University, Tehran, Iran

[2] Young Researchers and Elite Club, West Tehran Branch, Islamic Azad University, Tehran, Iran

[3] Centre for Asset Integrity Management, University of Pretoria, Pretoria, South Africa

[4] Department of Physics, K.N. Toosi University of Technology, P.O. Box 15875-4416, Tehran, Iran

[5] Department of Physics, Payame Noor University, P. O. Box 19395-3697, Tehran, Iran

The non-equilibrium conditions of these growth models lead to generation of the rough interfaces/surfaces. After generation of (2 + 1) dimensional interfaces using the mentioned two different growth models, they were used separately as the interfaces of MTJs. Here, the generated rough interfaces have been used for top interfaces of double barrier tunneling structures where the incident side is left to right. The results for transport properties of each MTJs have been compared. Also in the present work, the variation of temperature has been investigated on the spin-polarized electron transport through the MTJs.

The paper is organized as follows. At first, the model and formalism are described in Section 2. Then, the results and discussions are presented in Section 3, and at the end, the Section 4 devotes to conclusion and remarks.

2 Model and Formalism

Consider a system consisting of NM/EuS/NM/EuS/NM. The incident electrons propagate from left electrode to the right. The electric current entering the right electrode/collector is spin polarized because the tunneling electrons see different paths, namely spin-up and spin-down channels, depending on the spin of electrons. In other words, the spin-dependent transport is a consequence of imbalance between spin-up and spin-down currents that tunnel from the FMS electrode into a magnetic tunnel barrier. The barrier heights ($\varphi_\uparrow$, $\varphi_\downarrow$) are spin- and temperature-dependent and can be defined at below and above the magnetic ordering temperatures, T_c, as [3]:

$$\begin{cases} \varphi_\uparrow = \varphi_0 - \Delta E\sqrt{1-\dfrac{T}{T_c}}, & T \le T_c, \\ \varphi_\downarrow = \varphi_0 + \Delta E\sqrt{1-\dfrac{T}{T_c}}, & T \le T_c, \\ \varphi = \varphi_0, & T > T_c, \end{cases} \tag{1}$$

where $T_c = 16.5$ K, $\Delta E = 0.36$ eV is the spin-splitting energy between the two spin sub bands in the FMS layer at zero temperature, and $\varphi_0 = 0.75$ eV is the energy difference between the bottom of the conduction bands in the FMS layer and that of the NM electrode at zero temperature and zero bias voltage [11, 12].

For electrons propagating through the NM/FMS/NM/FMS/NM magnetic tunnel junction, the effective one-electron Hamiltonian in the z-direction is given by

$$H = \frac{-\hbar^2}{2m_j^*}\frac{d^2}{dz^2} + V_j(r_\parallel, z) + V_j^\sigma \quad , \quad \mathrm{j} = 1\text{–}5 \tag{2}$$

where m_j^* is the effective mass in each region and

$$V_j(r_\parallel, z) = \begin{cases} 0, & z < 0 \\ E_F + V(r_\parallel, z) - \dfrac{eV_a}{4}, & 0 < Z < b \\ -\dfrac{eV_a}{2}, & b < Z < b + c \\ E_F + V(r_\parallel, z) - \dfrac{3eV_a}{4}, & b + c < Z < b + c + d \\ -eV_a, & Z > b + c + d \end{cases} \tag{3}$$

where b, d, and c are the thicknesses of the two barriers and the central layer, respectively. E_F is the fermi energy, V_a is the bias voltage, and $r_\parallel = (x, y)$ is the in-plane coordinate vector. $V(r_\parallel, z) = \phi_0[\theta(z - f(r_\parallel))]$, where $\theta(z)$ is the step function and $f(r_\parallel)$ is the width of the rough interfaces [30]. If $f(r_\parallel)$ becomes zero, the transmission through perfect planar interfaces will label by perfect component. It is worthy to note that the first and third interfaces are considered rough. The last term in Eq. (2) is a spin-dependent potential and denotes the s–f exchange coupling between the spin of tunneling electrons and the localized f spins in the FMS layers [31–33]. Within the mean-field approximation, V_j^σ is proportional to the thermal average of the f spins, $\langle S_z \rangle$ (7/2 Brillouin function), and can be written as $-I\sigma\langle S_z\rangle$ and $-I\eta\langle S_z\rangle$ for the left and right FMS barriers, respectively. Here, $\eta = +1(-1)$ for the parallel (antiparallel) alignment of the magnetizations. Also, I is the s–f exchange constant in the magnetic barrier, and $\sigma = \pm 1$ for spin-up and spin-down electrons [11].

The wave function is written as

$$\psi_j = \sum_q \left(a_{j\sigma}^\gamma(q) e^{(ik_j z)} + b_{j\sigma}^\gamma(q) e^{-(ik_j z)} \right) e^{(i\boldsymbol{q}\cdot\boldsymbol{r}_\parallel)}, \tag{4}$$

in each region. $q = (q_x, q_y)$ is the transverse wave vector, k_j is the wave number in the jth region, and $r_\parallel = (x, y)$ is the in-plane coordinate vector. $a_{j\sigma}^\gamma(q)$ and $b_{j\sigma}^\gamma(q)$ correspond to forward and backward propagation states, respectively, where $\gamma = 0$ and ± denote to direct and scattered components. Here, we used the transfer matrix:

$$\begin{bmatrix} a_{5\sigma}^{(+)} \\ a_{5\sigma}^{(0)} \\ a_{5\sigma}^{(-)} \\ 0 \\ 0 \\ 0 \end{bmatrix} = M \begin{bmatrix} 0 \\ a_{1\sigma}^{(0)} \\ 0 \\ b_{1\sigma}^{(+)} \\ b_{1\sigma}^{(0)} \\ b_{1\sigma}^{(-)} \end{bmatrix} \tag{5}$$

where $a_{1\sigma}^{(\pm)} = 0$ denotes that there is only the direct incident component [12, 34]. Also, we have considered $b_{5\sigma}^{(\gamma)} = 0$ since there is no reflection in the last region across the interface. The transmission through the double barrier heterostructure can be calculated by the continuity conditions of wave function ψ and the probability current density of the electron $(1/m^*)(d\psi/dz)$, as follows:

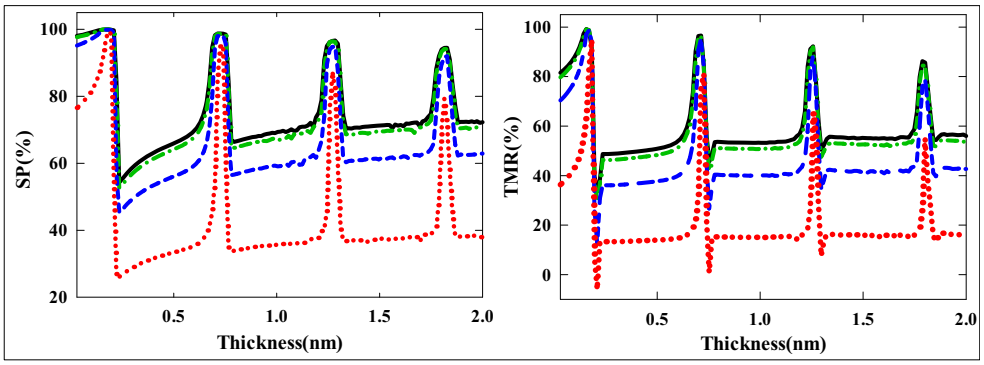

Fig. 1 Central layer thickness and temperature dependency of SP and TMR for perfect case (T = 0, 0.3 T_c, 0.6 T_c, and 0.9T_c from top to down)

$$T_{\sigma}^{(\gamma)}(E_z, V_a) = \frac{k_5^{(\gamma)}}{k_1^{(\gamma)}} \frac{m_1^*}{m_5^*} \left| \frac{a_{5\sigma}^{(\gamma)}}{a_{1\sigma}^{(\gamma)}} \right|^2, \tag{6}$$

Total transmission is achieved by $T_{tot} = \sum_{\gamma} T^{(\gamma)}$ where $\gamma =$ 0 and ± refer to the direct and indirect (roughness scattered) components of transmission probability, respectively [12]. Therefore, the current density can be written as [31],

$$j(V_a) = \frac{em^* k_B T}{4\pi^2 \hbar^3} \int_0^{\infty} T_{\sigma}^{\gamma}(E_z, V_a) \ln \left[\frac{1 + \exp\left[{(E_F - E_z)}/{k_B T} \right]}{1 + \exp\left[{(E_F - E_z - eV_a)}/{k_B T} \right]} \right] dE_z, \tag{7}$$

where T_{σ}^{γ} (E_z, V_a) is the transmission probability. Spin polarization is obtained from current densities of spin-up (↑) and down (↓) orientations, SP= $\frac{j_{\uparrow} - j_{\downarrow}}{j_{\uparrow} + j_{\downarrow}}$ [7, 8]. Consequence of spin-

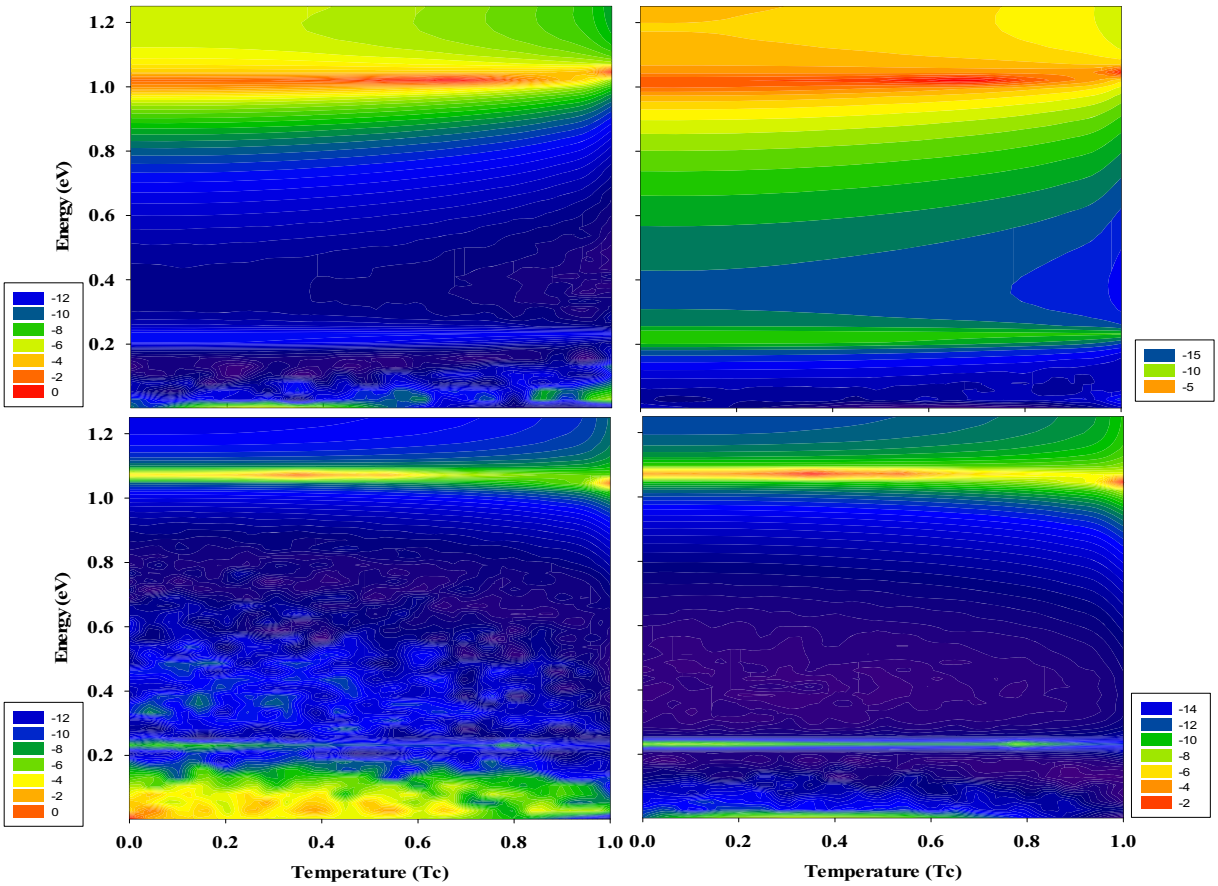

Fig. 2 Logarithm of transmission probability as a function of incident electron energy in the presence of roughness for an interval of temperatures. The top and bottom figures are related to spin-up and down orientation, respectively. The right and left columns show the effect of BD and RD roughness models, respectively

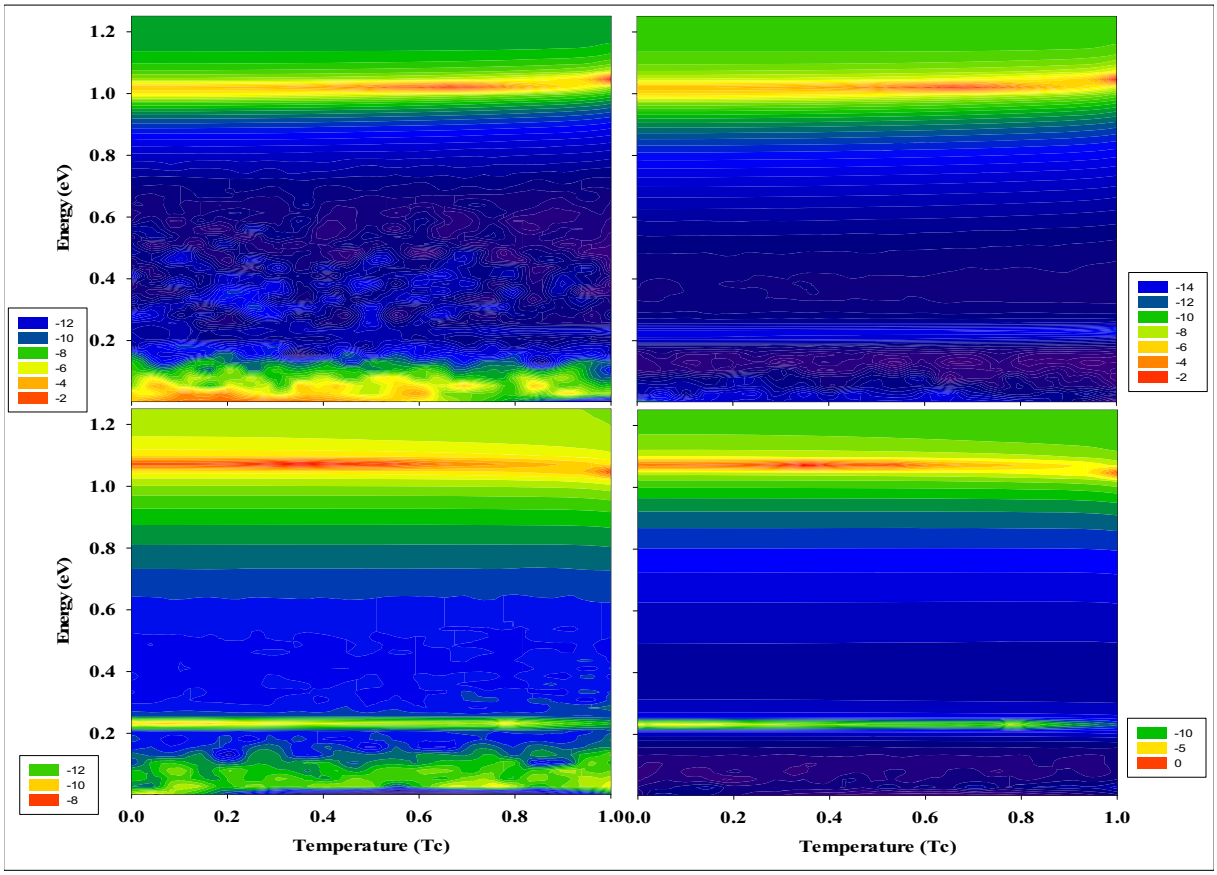

Fig. 3 Logarithm of transmission probability as a function of incident electron energy in the presence of roughness for an interval of temperatures. The top and bottom figures are related to spin-up and down orientation, respectively. The right and left columns show the effect of BD and RD roughness models, respectively

dependent tunneling is an important effect, TMR. Majority of researchers define TMR as the conductance difference between parallel (P) and antiparallel (AP) magnetizations of ferromagnetic regions, normalized by the antiparallel conductance, i.e. TMR $= \frac{J_P - J_{AP}}{J_{AP}}$ [7, 8].

3 Results and Discussion

The values of the used parameters are as follows. The thicknesses of barriers and quantum well are considered 0.5 and 0.75 nm, respectively. We consider $m_1 = m_0$ and $m_2 = 1.5m_0$ [35] for the electron effective mass in NM and FMS materials, respectively, where m_0 is the electron mass in free space [11]. Also, E_F is the electron Fermi energy which has been taken as 1.25 eV. The parameters for EuS barrier layer are $I = 0.1$ eV and $S = 7/2$ [36]. The $T_c = 16.5$K [37].

Reduction of effective barrier thickness and decrease of transport is the general description of roughness effect in electron transport phenomena. In spin filter junctions, there are two conduction channels, one for each spin. As it was mentioned before, the barrier heights are temperature-dependent. Thus, based on Eq. (1), the spin-up barrier height decreases with the decreasing temperature. Also, above T_c, two spin channels see the same barrier height, therefore, the SP and TMR reduce to zero [1, 2]. In order to understand the origin of peaks and periodic variation of electric current in SP and TMR, the energy dependency of the transmission probability through MTJs is analyzed. In calculation, the applied voltage is $V_a = 50$ mV [12]. The other parameters are mentioned in the figures. Figure 1 shows the dependency of SP and TMR to thickness of central layer for different temperatures. Several features of The SP and TMR curves are interesting. There are well-defined peaks which decrease with increasing the thickness of the central layer of double barrier structure. This behavior is a result of resonant tunneling through structure and quantum-well states formed in the central layer. Also, the periodicity in SP and TMR is correlated strongly with the resonant states in quantum wells [11, 13, 14, 31]. In previous works, the perfect case for MTJs and their results are studied [11, 12, 32]. In the present work, effect of interfacial roughness type on tunneling phenomena was interesting; thus, the transmission probabilities as a function of incident electron energy have been shown for all spin orientations and all configurations.

Also, as the barriers were considered ferromagnetic semiconductor materials, the effect of temperature variation has

been investigated. In tunneling phenomena, an electron impinging on structure has a maximum quantum tunneling probability when its energy corresponds to a quasi-bound. Because of the quasi-bound states in the central NM layer, the transmission coefficients reach unity at the resonance peaks which become sharper in the low incident energy region, since in this energy region, the resonance levels are more strongly quantized [11]. In no perfect cases (considering rough interfaces), there are resonant peaks in transmission probabilities that do not reach unity. This fact can be seen in Figs. 2 and 3 for all spin orientations and configurations.

Further analysis of transmission curves is noteworthy because the type of roughness has the significant effect on the conduction. The results indicate that the interface roughness scattering reduces the resonant tunneling peak and this reduction is different for various interface roughness types. We have considered two different MTJs which their top rough interfacials were produced by using the BD and RD models, respectively. The sampling phase detector (SPD) tunneling through two MGJs has been compared in Figs. 2 and 3. The electron scattering effect due to rough interfaces, which are produced by using the random deposition model, is stronger than that of the ballistic ones.

The same results for all spin orientations and antiparallel configuration are presented in Fig. 3. Also, in this figure, the electron scattering through the tunneling structures, which their interfaces are generated with RD model, is more than that of the BD ones.

Based on Eq. (7), the current density is related to transmission probability and temperature [11, 12]. There is an imbalance between current density of spin-up and down orientation which causes TMR and SP phenomenon. Figure 4 shows the thickness and temperature dependency of SP and TMR of SPD tunneling through rough MTJs. The tunneling phenomena through rough interfaces can cause spin flip effect, so some of the majority of the electrons change their spin direction and tunnel into the

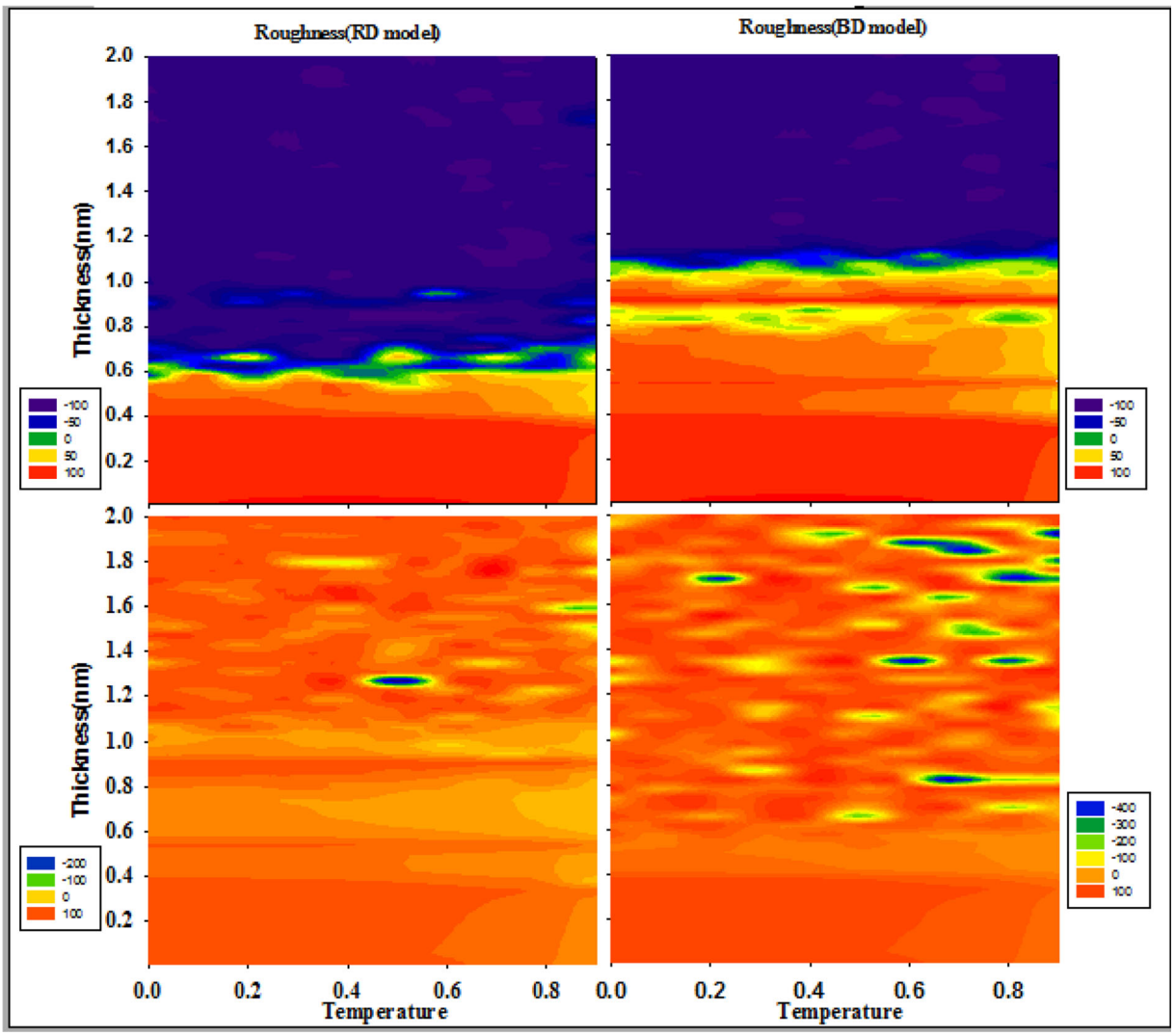

Fig. 4 Thickness and temperature dependency of SP (top figures) and TMR (bottom figures)

corresponding minority states. Therefore, asymmetry distribution of the density of states may be decreased.

On the other hand, the scattering process can create the additive dip, and peak resonance energies and their position may be changed with variation of central layer width. These facts cause irregularity in SP and TMR behavior. With increasing the temperature, the SP and TMR magnitude decrease [33]. This is because of temperature dependency of spin-splitting conduction band of spin-filtering barriers. In another words, as temperature decreases, the spin channel with the lower barrier height has a larger tunneling probability. At $T = 0K$, the TMR and spin polarization have their maximum values and above the T_c, splitting of conduction bands becomes zero [1, 2]. These effects can be seen in no perfect case too, but the presence of roughness suppresses the temperature dependence [38–45].

These results are in agreement with experimental studies and indicate that besides the temperature, barrier thickness, and height, the type and magnitude of roughness play the critical role for controlling the tunneling through MTJs [17, 18, 38]. These results could be useful for designing the spin filter devices and experimental research.

4 Conclusion

In present work, the effects of two different types of interface roughness and temperature have been studied on the spin-filtering process through spin filter tunneling. The presence of rough interfaces causes reduction of maximum achievable resonant tunneling and also results to the reduction of spin-filtering efficiency. As a noteworthy result which agrees with the experimental ones, the electron scattering effect due to rough interfaces, which are produced by using the random deposition model, is stronger than that of the ballistic ones. Also, based on numerical results, roughness suppresses the temperature dependency of transport properties of spin-filtering structures.

References

1. Ovchinnikov, S.G., Orlov, Y.S., Nikolaev, S.V., et al.: Phys. Solid State. **60**, 1177 (2018). https://doi.org/10.1134/S1063783418060276
2. Ovchinnikov, S.G., Orlov, Y.S., Dudnikov, V.A., Vereschagin, S.N., Perov, N.S.: J. Magn. Magn. Mater. **383**, 162–165 (2015)
3. Gavrichkov, V.A., Polukeev, S.I., Ovchinnikov, S.G.: J. Exp. Theor. Phys. **127**, 713 (2018). https://doi.org/10.1134/S1063776118100023
4. Orlov, Y.S., Nikolaev, S.V., Nesterov, A.I., et al.: JETP Lett. **105**, 771 (2017). https://doi.org/10.1134/S0021364017120104
5. Gholipur, R., Bahari, A.: Mater. Chem. Phys. **180**, 135–143 (2016). https://doi.org/10.1016/j.matchemphys.2016.05.053
6. Poulopoulos, P., et al.: Applied Physics Letters. **104**(11), 112411–112411-4 (2016)
7. Tsymbal, E.Y., NMryasov, O., Le Clair, P.R.: J. Phys.: Condens. Matter. **15**, R109–R142 (2003)
8. Zŭtić, I., Fabian, J., Sarma, S.D.: Rev. Mod. Phys. **76**, –410 (2004, 323)
9. Kalitsov, A., Zermatten, P., Bonell, F., Gaudin, G., Andrieu, S., Tiusan, C., Chshiev, M., Velev, J.P.: J. Phys. Cond. Mat. **25**, 496005 (2013)
10. Waldron, D., Timoshevskii, V., Hu, Y., Xia, K., Guo, H.: Phys. Rev. Lett. **97**, 226802 (2006)
11. Saffarzadeh, A.: J. Phys. Condens. Matter. **15**, 3041–3051 (2003)
12. Farhad Masoudi, S.: Zhaleh Ebrahiminejad. Surf. Sci. **630**, 85–88 (2014)
13. Chshiev, M., Stoeffler, D., Vedyayev, A., Ounadjela, K.: Europhys. Lett. **58**, 257 (2002)
14. Kalitsov, A., Coho, A., Kioussis, N., Vedyayev, A., Chshiev, M., Granovsky, A.: Phys. Rev. Lett. **93**, 046603 (2004)
15. Belashchenko, K.D., Tsymbal, E.Y., van Schilfgaarde, M., Stewart, D.A., Oleynik, I.I., Jaswal, S.S.: Phys. Rev. B. **69**, 174408 (2004)
16. Heiliger, C., Zahn, P., Yavorsky, B.Y., Mertig, I.: Phys. Rev. B. **72**, 180406(R) (2005)
17. Miller, C.W.: J. Magn. Magn. Mater. **321**, 2563–2565 (2009)
18. Miller, C.W., Belyea, D.D.: J. Appl. Phys. **105**, 094505–1–094505-5 (2009)
19. Barabasi, A.L., Stanley, H.E.: Fractal Concepts in Surface Growth. Cambridge University Press, New York (1995)
20. Hoseinzadeh, S., Ghasemiasl, R., Bahari, A., et al.: Journal of Elec Materi. **47**, 3552 (2018). https://doi.org/10.1007/s11664-018-6199-4
21. Hoseinzadeh, S., Ghasemiasl, R., Bahari, A., et al.: J. Mater. Sci. Mater. Electron. **28**, 14446 (2017). https://doi.org/10.1007/s10854-017-7306-7
22. Hoseinzadeh, S., Ghasemiasl, R., Bahari, A., et al.: J. Mater. Sci. Mater. Electron. **28**, 14855 (2017). https://doi.org/10.1007/s10854-017-7357-9
23. Hoseinzadeh, S., Ramezani, A.H.: J. Nanoelectron. Optoelectron. **14**, 1413–1419 (2019). https://doi.org/10.1166/jno.2019.2564
24. Ramezani, A.H., Hoseinzadeh, S., Sari, A.: H. **14**(3), 425–430 (2019). https://doi.org/10.1166/jno.2019.2527
25. Hoseinzadeh, S., Ramezani, A.H.: J Nanostruct. **9**, 276–286 (2019). https://doi.org/10.22052/JNS.2019.02.010
26. Ramezani, A.H., Hoseinzadeh, S., Bahari, A.: J. Inorg. Organomet. Polym. **28**, 847 (2018). https://doi.org/10.1007/s10904-017-0769-4
27. Najafi-Ashtiani, H., Bahari, A., Gholipour, S., et al.: Appl. Phys. A Mater. Sci. Process. **124**, 24 (2018). https://doi.org/10.1007/s00339-017-1412-5
28. Pahlavan, A., Bahari, A.: The first quantization of spin field in de Sitter Space. Int. J. Theor. Phys. **48**, 1449–1459 (2009)
29. Hoseinzadeh, S., Ramezani, A.H.: J. Chin. Soc. Mech. Eng. **39**, 501–507 (2018)
30. Shokri, A.A., Ebrahiminejad, Z.H., Masoudi, S.F.: Thin Solid Films. **519**, 2193–2200 (2011)
31. Wilczynski, M., Barnas, J.: J. Magn. Magn. Mater. **221**, 373–381 (2000)
32. Bai, C., Zhang, X.: Phys. Lett. A. **372**, 725–729 (2008)
33. Xu, P.X., Karpan, V.M., Xia, K., Zwierzycki, M., Marushchenko, I., Kelly, P.J.: Phys. Rev. B. **73**, 180402–1–180402-4 (2006)
34. Liu, H.C., Coon, D.D.: J. Appl. Phys. **64**, 6785–6789 (1988)
35. Baum, G., Kisker, E., Mahan, A.H., Raith, W., Reihl, B.: Appl. Phys. **14**, 149–153 (1977)
36. Nolting, W., Dubil, U., Matlak, M., Phys, J.: C: Solid State Phys. **18**, 3687 (1985)
37. P. Wachter 1979 Handbook on the physics and chemistry of rare earths ed K A Gschneider and LEyringJr (Amsterdam: North-Holland) ch 19

38. Miller, C.W., Li, Z.-P., Schuller, I.K., Dave, R.W., Slaughter, J.M., Akerman, J.: Phys. Rev. B. **74**, 212404–1–212404-4 (2006)
39. Dastan, D., Londhe, P.U., Chaure, N.B.: J. Mater. Sci. Mater. Electron. **25**, 3473 (2014). https://doi.org/10.1007/s10854-014-2041-9
40. Dastan, D.: Appl. Phys. A Mater. Sci. Process. **123**, 699 (2017). https://doi.org/10.1007/s00339-017-1309-3
41. Dastan, D., Panahi, S.L., Chaure, N.B.: J. Mater. Sci. Mater. Electron. **27**, 12291 (2016). https://doi.org/10.1007/s10854-016-4985-4
42. Dastan, D., Banpurkar, A.: J. Mater. Sci. Mater. Electron. **28**, 3851 (2017). https://doi.org/10.1007/s10854-016-5997-9
43. Sangashekan, M., Asan, S., Gilani, H.G.: Fibers Polym. **20**, 1411 (2019). https://doi.org/10.1007/s12221-019-8542-7
44. Bahari, A., Babaeipour, M., Soltani, B.: J. Mater. Sci. Mater. Electron. **27**, 2131 (2016). https://doi.org/10.1007/s10854-015-4002-3
45. Hoseinzadeh, S., Heyns, P. and Kariman, H. (2019), Int.J Num. Methods.Heat Fluid Flow, ahead-of-print. https://doi.org/10.1108/HFF-06-2019-0485